AIP | Conference Proceedings

Silo clogging reduction by placing an obstacle above the outlet

C. Lozano, I. Zuriguel, A. Janda, A. Garcimartín, R. Arévalo et al.

Additional information on AIP Conf. Proc.

Silo Clogging Reduction by Placing an Obstacle Above the Outlet

C. Lozano*, I. Zuriguel*, A. Janda*, A. Garcimartín*, R. Arévalo† and D. Maza*

*Departamento de Física y Matemática Aplicada, Facultad de Ciencias, Universidad de Navarra, 31080 Pamplona, Spain.
†CNR-SPIN, Dipartimento di Scienze Fisiche, Università di Napoli 'Federico II', Naples, Italy

Abstract. We present an experimental study of the effect that an obstacle above the outlet of a silo has on the clogging probability. Both, the size of the orifice and the obstacle position are varied for a chosen obstacle size and shape. If the position of the obstacle is properly selected the clogging probability can be importantly reduced. Indeed, as the outlet size is increased – and we approach the critical size above which there is not clogging – the obstacle effect is enhanced. For the largest outlet size studied, the clogging probability is reduced by a factor of more than one hundred. We will show, using numerical simulations, that the physical parameter behind the reduction of the silo clogging seems to be the decrease of the vertical pressure at the outlet proximities.

Keywords: Clogging, jamming, silo, obstacle, insert, arching
**PACS:** 45.70.Mg

INTRODUCTION

Granular flows are prone to clog when the outlet size is not much larger than the characteristic particle size. This behavior is observed in industrial granular flows [1, 2, 3, 4, 5, 6], traffic flows [7] or people escaping from a room under panic [8]. Despite the different nature of the particles in all these cases, we can observe strong similarities in their collective behavior. A number of studies consider the clogging events in the discharge of a silo in 3D [4, 5] and in 2D [2, 3, 6]. When spherical particles are used, the most important factor determining clogging is the relationship between the diameter of the particles and the outlet size. For the 3D case, it seems clear that there is a critical outlet size of around 5 times the size of the particles, above which clogging does not occur. For a given outlet and particles size, the distribution of avalanche sizes s (defined as the number of particles fallen between two successive clogs) displays an exponential decay. This exponential can be understood defining p as the probability that a particle passes through the outlet without forming a blocking arch [4]. Then, assuming that p is constant during the whole avalanche, the distribution of avalanche sizes can be written as $n(s) = p^s(1-p)$, where $1-p$ is the probability that a particle forms an arch that blocks the orifice. The first moment of this distribution is $\langle s \rangle = p/(1-p)$. This implies that the clogging phenomenon can be described by a characteristic parameter, $\langle s \rangle$, which depends on the orifice size. This allows us to collapse the histograms of s into a single plot using the rescaled variable $s/\langle s \rangle$.
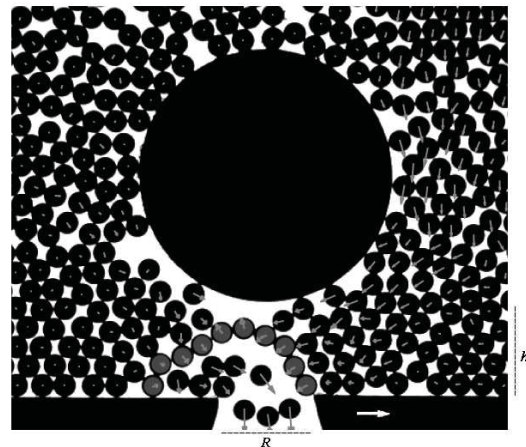
FIGURE 1. Photograph of the particles flowing out the silo. The vector velocities are plotted with grey arrows. The arrow in the bottom of the silo is the scale and corresponds to 100 mm/s. R is the length of the outlet and h the distance from the obstacle to the orifice. Particles conforming a possible arch that is not stabilized are plotted in gray.

An alternative parameter that can be used to characterize the ability of a system to develop clogs is the clogging probability (J_N). This is the probability that the flow of grains gets arrested before N beads fall out of the silo. This variable was firstly introduced by K. To. *et al.* [2] and subsequently related analytically with the mean avalanche size by Janda *et al.* [6]:
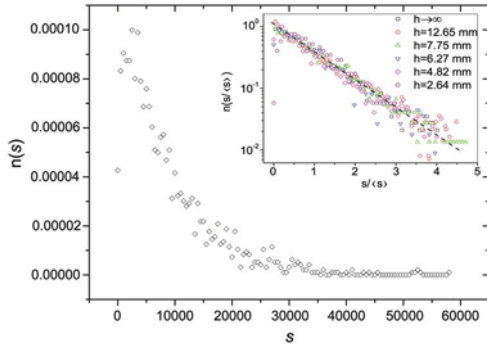
FIGURE 2. Histogram of the number of particles in an avalanche s. Data correspond to $R = 4.20$ mm and $h = 4.82$ mm. Inset: semilogarithmic plot of the avalanche size distributions rescaled by the mean avalanche size, for $R = 4.20$ mm and different obstacle positions as indicated in the legend. The dashed line indicates the exponential behavior.

$$J_N(R) = 1 - (\langle s \rangle / (1 + \langle s \rangle))^N \qquad (1)$$

Since the 1960's, empirical placement of inserts or obstacles above the outlet has been used in silo design to modify the internal flow of the particles converting funnel flow to mass flow [9]. Alternatively, studies on crowd dynamics have shown that an obstacle properly placed in front of the exit may lead to a reduction of the evacuation time in panic situations [10].

In a recent paper we studied the effect of placing an obstacle above the outlet of a silo with a fixed size $R = 4.2$ *mm* [11]. If the position of the obstacle is properly selected, the avalanche size can be reduced by a factor close to 100. The aim of this research is to study the effect of the obstacle position in the clogging probability, J_N, for different outlet sizes. The first noticeable fact is that the clogging probability changes dramatically with h, without any significative alteration of the flow rate. We propose that the insert reduces the pressure in the region of arch formation, being this the main cause of clogging reduction.

EXPERIMENTAL SETUP

The experimental setup consists of a two-dimensional rectangular silo made of two sheets of glass (800 *mm* hight and 200 *mm* wide). The gap between the two sheets is 1.1 mm, and we filled it with stainless-steel beads of 1.00 ± 0.01 mm conforming a monolayer. The flat bottom of the silo is formed by two facing metal pieces, so that their edges define the outlet size R which can be varied at will. A circular obstacle of 10 mm diameter is placed above the orifice as shown in Fig.1. The distance

from the bottom of the obstacle to the outlet (h) can be changed and is measured with an approximate error of 0.05 mm. Henceforth, the case of a silo without obstacle will be referred to as $h \to \infty$. We measure the avalanche sizes s for different obstacle positions and for three different outlet sizes ($R = 3.13, 4.20, 4.55$ mm). We have chosen these values of R to cover a wide range of mean avalanche sizes $\langle s \rangle$ for the case of the silo without obstacle: from $\langle s_{h \to \infty} \rangle = 100$ to $\langle s_{h \to \infty} \rangle = 3000$ particles.

The protocol is the following. First of all, the silo is filled by pouring the grains along its whole width through a hopper at the top. After that, the exit is opened and grains start to flow through the outlet till an arch clogs it. The beads are collected in a cardboard box placed on a balance which allows the measurement of the avalanche size s, which is given in number of beads. Then, the flow is restarted by blowing a jet of compressed air aimed the orifice. The silo is refilled whenever the level of grains falls below a fixed threshold of around 300 *mm* (1.5 times the width of the silo). This is accomplished in order to avoid big changes in the pressure at the bottom. For each obstacle position, between 800 and 3000 avalanches were obtained. Additionally, for each experimental conditions we recorded movies of the region above the outlet at 1500 frames per second during a total lapse of 40 seconds.

RESULTS

The first quantity that we analyze is the avalanche size s. We show that, regardless of the obstacle position, the distribution of s decays exponentially (Fig.2). As mentioned previously, this exponential decay allows a meaningful rescaling of the distributions obtained in different situations (inset of Fig.2). The only noteworthy difference between the distributions for different values of h is the value of mean avalanche size $\langle s \rangle$. Hence, the clogging probability will depend on the obstacle position (recall that the mean avalanche size $\langle s \rangle$ is related to the clogging probability J_N by equation 1).

In order to obtain the maximum advantage of the obstacle (in terms of reducing the clogging probability) it is crucial to place it properly. When it is placed at the optimal distance to the exit orifice, the obstacle can reduce the probability of clogging by two orders of magnitude. Although this amount changes depending on the orifice size, there is always a marked minimum for J_N at a given h. In Fig.3, we present the experimental values of J_N (for $N = 100$ $N = 200$ and $N = 1000$) versus h for three different values of R. These plots manifest that the jamming probability as a function of h displays the same trend independently of the outlet size R and the number of particles N selected to define J_N. Let us first explain this trend focusing in a single curve: for exam-
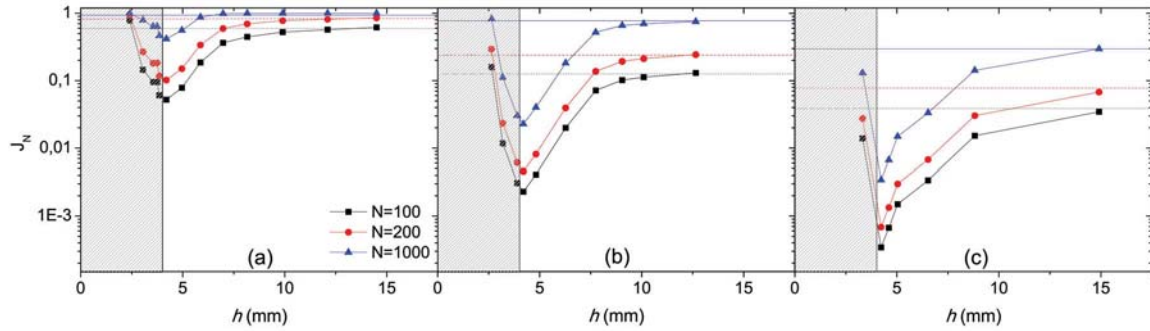
FIGURE 3. The clogging probability J_N as function of h for different outlet sizes (a) $R = 3.13$ mm, (b) $R = 4.20$ mm, (c) $R = 4.55$ mm. The horizontal lines indicate the values of J_N when $h \to \infty$. The region $h < 4$ mm is in gray, signaling the different nature of the clogging process for such obstacle positions.
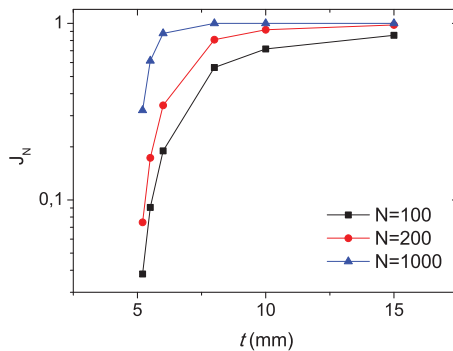
FIGURE 4. The jamming probability J_N as function of layer thickness t for a silo without obstacle and an outlet size $R = 3.5$ mm.

ple J_{100} for $R = 4.2$ (squares in Fig.3b). If the obstacle is too far from the exit ($h > 10$), the value of J_N is quite close to the case of a silo without obstacle (indicated in Fig.3b by an horizontal line). Then, approaching the obstacle to the outlet (reducing h) leads to a reduction of J_N until a minimum is reached for $h \approx 4mm$. Notice that the plot is in semilogarithmic scale, so the minimum is very conspicuous. Indeed, the value of J_N for this particular case is reduced almost 100 times with respect to the case without obstacle. For $h < 4mm$ the jamming probability increases again due to the formation of arches between the obstacle and the silo bottom [11]. This regime is not ruled by R but by the distance between the obstacle and the bottom, which is indeed the narrowest passage. To indicate that clogging in this region has a completely different nature, we have grayed the zone of $h < 4mm$ in Fig. 3. These types of arches have been also observed in other studies of silos with oblique exits [12] and pedestrian flows through obstacles [13].

The curves obtained for different values of N, namely $N = 100$, 200 and 1000 particles, are all very similar although, as expected, J_N increases with N. Modifying the outlet size (R) also leads to similar shapes of the curves. In this case it is noticeable that the minimum is enhanced as R increases. Effectively, as R approaches the supposed value above which clogging is not possible ($R \approx 8$ in 2D) [6], the effect of the obstacle is magnified. This result suggests that the small perturbations introduced by the obstacle have more consequence as the critical point is approached.

In order to understand the significative change in the jamming probability induced by the obstacle, the flow rate (defined as the number of particles that pass through the outlet per unit time) was studied [11, 14]. Surprisingly, the mean flow rate is not significatively dependent on the obstacle position, yet values up to 10% higher than in a silo with obstacle can be reached. This small effect of the obstacle on the flow rate also appears in previous studies carried out in silos with large orifices [15, 16], far from the region of clogging. We also measured the velocity of the particles above the outlet revealing, for the case of silo with obstacle, the apparition of negative velocities in the vertical direction, i.e. particles that move upwards in the region of arch formation. In Fig. 1, we present a snapshot of the particles flowing through the outlet with the vector velocities plotted with gray arrows. Clearly, at this specific moment, the two uppermost particles shaded in gray are moving upwards. This behavior is not observed when the obstacle is absent. Therefore, we speculate that the reduction of the jamming probability induced by the obstacle could be related with the apparition of these upwards ejections of particles. Effectively, it seems reasonable that if a number of particles coincide above the orifice forming an arch (see for example the shaded particles in Fig. 1), the absence of more particles arriving behind them could prevent the stabilization of the arch as particles are ejected upwards. This idea is in-

700

spired in the dynamics of crowds passing through a bottleneck. If there is not panic, pedestrians are polite and conflicts (collisions) are quickly solved by backwards movements. Nevertheless, when panic is high, pressure increases and the resolution of conflicts is more difficult leading to an increase of clogging [13].

Based on these results of crowd dynamics, we propose that the mechanism by which the obstacle prevents clogging is a reduction of the pressure exerted to the particles in the region of arch formation. As experimental measurements of the pressure inside the granular bulk are complicated, we performed an alternative numerical experiment. This simulation consisted on measuring the jamming probability in silos without obstacle but filled with different number of particles. Then, we measured t, the layers thicknesses which one would get with an hexagonal packing, so that the pressure at the bottom of the silo varies with t. Note that as t increases the pressure could saturate due to the Janssen effect [17].

We have used soft particle molecular dynamics simulations of disks (diameter $d = 1$ mm) in two dimensions [18] which have been previously proved to nicely reproduce experimental results of the flow of particles through bottlenecks [19]. The simulated flat bottomed silo was $15d$ wide and had an outlet size $R = 3.5d$. The particles that left the silo were placed without kinetic energy on top of the upper layer of grains, so the total number of particles in the system was constant. When the flow is stopped due to the formation of a stable arch, the avalanche size is registered, and the flow is resumed by removing three particles that form the arch. The process was repeated till 3000 avalanches were obtained. We performed simulations for six different values of layer thickness t. The avalanche size distribution of the simulations decays exponentially regardless of the layer thickness. Hence the jamming probability J_N was calculated from the mean avalanche size using equation 1. In Fig.4 we show the results of J_N for different values of t. Clearly, it is revealed a strong dependence of the clogging probability on the layer thickness: the thinner the layer the smaller J_N. In addition, we observe an asymptotic behavior of J_N for high values of t that should be related with the pressure saturation. In summary, the behavior displayed in Fig.4 is in perfect agreement with the one presented in the Fig.3. Then, it can be concluded that the layer thickness t has a role similar to the obstacle position h, in terms of pressure reduction.

CONCLUSIONS

In this work, we have demonstrated that placing an obstacle above the outlet of a silo strongly affects to the clogging probability (J_N). If the position of the obstacle is properly selected, the clogging probability can be re-duced by a factor of more than one hundred. In addition, we show that the greater the outlet size is, the stronger the effect of the obstacle. Considering both, the experimental results and the numerical simulations, it seems clear that the physical mechanism responsible for the decreasing of the jamming probability is that the obstacle reduces the pressure above the outlet. This results in a reduction of the confinement of the particles preventing the stabilization of the arches.

ACKNOWLEDGMENTS

REFERENCES

1. R. M. Nedderman, *Statitcs and Kinematics of Granular Materials*, Cambridge University Press, Cambridge, 1992, pp. 322–328.
2. K. To, P.-Y. Lai, and H. K. Pak, *Phys. Rev. Lett.* **86**, 71 (2001).
3. K. To, and P.-Y. Lai, *Phys. Rev. E* **66**, 011308 (2002).
4. I. Zuriguel, L. A. Pugnaloni, A. Garcimartín, and D. Maza, *Phys. Rev. E* **68**, 030301 (2003).
5. I. Zuriguel, A. Garcimartín, D. Maza, L.A. Pugnaloni and J.M. Pastor, *Phys. Rev. E* **71**, 051303 (2005).
6. A. Janda, I. Zuriguel, A. Garcimartín, L. A. Pugnaloni and D. Maza, *Europhys. Lett.* **84**, 44002 (2008).
7. R. Vaughan, V. F. Hurdle, *Transpn. Rex-E* **26B**, 5 (1992).
8. D. Helbing, I. Farkas, T. Vicsek, *Nature* **407**, 6803 (2000).
9. J. R. Johanson, *Powder Technology* **1**, 6 (1968).
10. D. Helbing *et al.*, *Transportation Science* **39**, 1 (2005).
11. I. Zuriguel, A. Janda, A. Garcimartín, C. Lozano, R. Arévalo and D. Maza, *hys. Rev. Lett.* **107**, 278001 (2011).
12. H. G. Sheldon and D. J. Durian, *Granular Matter* **12**, 579 (2010).
13. G. A. Frank and C. O. Dorso, *Physica A* **390**, 2135 (2011).
14. C. Lozano, A. Janda, A. Garcimartín, D. Maza and I. Zuriguel, *Phys. Rev. E* **86**, 031306 (2012).
15. S. C. Yang and D. D. Hsiau, *Powder Technology* **120**, 244 (2001).
16. F. Alonso-Marroquin, D. I. Azeezullah, D. A . Galindo-Torres, and L. M. Olsen-Kettle. *Phys. Rev. E* **86**, 020301(R) (2012).
17. H. A. Janssen Versuche über Getreidedruck in Silozellen. Zeitschr. d. Vereines deutscher Ingenieure **39**, 1045 (1895).
18. R. Arévalo, D. Maza, and L. A. Pugnaloni, *Phys. Rev. E* 74, 021303 (2006).
19. C. Mankoc, A. Janda, R. Arévalo, J. M. Pastor, I. Zuriguel, A. Garcimartín and D. Maza, *Granular Matter* **9**, 407 (2007).